

# Measurement of Optical Two-Photon Gain in Electrically Pumped AlGaAs at Room Temperature

Amir Nevet,\* Alex Hayat, and Meir Orenstein

*Department of Electrical Engineering, Technion, Haifa 32000, Israel*

(Received 21 October 2009; published 20 May 2010)

We demonstrate experimentally two-photon gain in semiconductor structures, shown previously only in dilute atomic systems. Two-photon gain is directly observed and characterized in electrically pumped room-temperature semiconductor devices, in good agreement with theory. The semiconductor structure was designed to enhance the two-photon interaction and reduce parasitic effects. The nonlinear two-photon amplification is studied directly by examining the current dependence of the optical intensity growth, and indirectly by monitoring the reduction in one-photon emission due to two-photon transitions above transparency.

DOI: 10.1103/PhysRevLett.104.207404

PACS numbers: 78.45.+h, 42.50.Hz, 78.60.Fi

Two-photon stimulated emission was proposed in the early days of the laser aimed at the development of alternative kinds of quantum oscillators [1,2]. Two-photon amplifiers and lasers exhibit unique classical behavior such as bistability and giant pulse generation [2] as well as quantum properties including squeezing [3] due to the inherent nonlinearity of the process [4]. Efficient two-photon sources can, therefore, contribute to various fields of science and technology, from high-power applications, such as multiphoton biomedical microscopy, to a range of quantum applications exploiting nonclassical squeezed light such as continuous variable quantum information processing [5].

Spontaneous two-photon emission (TPE) results from a second-order electron transition between energy levels, simultaneously emitting a pair of photons [Fig. 1(a)], and is significant in different realms of science including atomic physics and astrophysics [6]. In fully (doubly) stimulated TPE, necessary for two-photon gain (TPG), a photon pair stimulates the emission of another pair [Fig. 1(c)], in contrast to singly stimulated TPE where one incident photon is duplicated and a complementary-energy photon is spontaneously emitted [Fig. 1(b)]. A decade after the observation of singly stimulated TPE [7], fully stimulated TPE was observed [8], leading to the demonstration of a two-photon laser (TPL) [9]. All previous TPL experiments were performed on discrete-level atomic systems in a maserlike configuration, where atoms were injected into a very high-quality cavity. Despite the significant advancements in TPL research, the powers emitted from such TPL schemes are relatively low, primarily due to the small numbers of interacting atoms. Furthermore, the optical pumping of atomic TPLs limits the available intracavity intensity due to competing nonlinear effects such as self-focusing, stimulated anti-Stokes Raman scattering, and parametric wave mixing involving the pump field, thus requiring sophisticated orthogonal beam configurations [10].

Semiconductors, having orders of magnitude higher carrier concentrations, can provide a compact high-power

alternative to the atomic maser-type configurations. Moreover, contemporary mature semiconductor fabrication technology allows engineering of energy bands, tight-confinement waveguiding for long nonlinear interaction, and electrical pumping, enabling the realization of miniature efficient devices. Two-photon gain in semiconductors was proposed theoretically [11] and its suitability for some applications including TPLs [12] and pulse compression has been examined both analytically and numerically [13,14]. Recently, spontaneous and singly stimulated TPE in semiconductors were observed [15] exhibiting

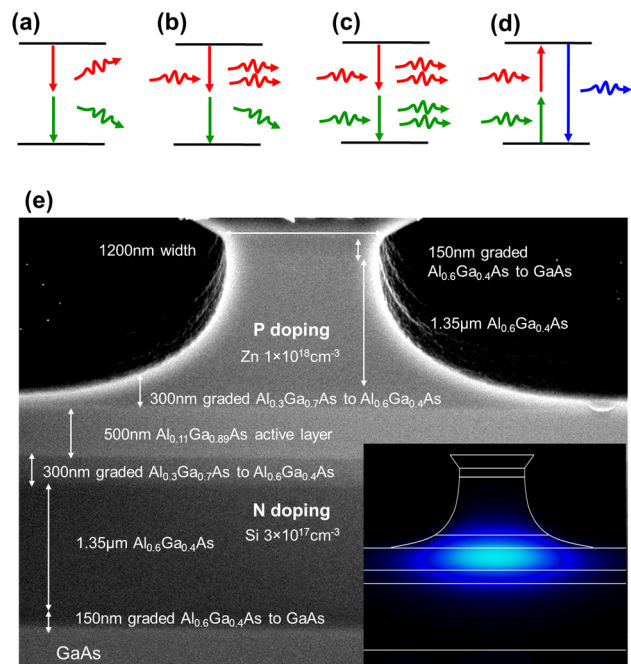


FIG. 1 (color online). (a) Electron transition diagram of spontaneous TPE, (b) singly stimulated TPE, (c) fully (doubly) stimulated TPE (TPG), and (d) two-photon absorption induced luminescence. (e) Scanning electron microscope image of the ridge waveguide. The inset is a beam propagation simulation of the fundamental mode for wavelength of  $1.56 \mu\text{m}$ .

features in accordance to a newly developed theory [16]. In contrast to semiconductor two-photon absorption (TPA), which has been substantially investigated and is widely employed [17–19], the opposite processes of TPG in semiconductors was not observed before. The standard modern semiconductor laser structures based on quantum wells appear to be unsuitable for efficient TPG due to the very small confinement of the optical mode to the active region [20]; however, they were shown to be sufficient for achieving two-photon transparency (TPT) under current injection [21].

Here we report the first experimental observation of TPG in semiconductors. The phenomenon is demonstrated in an electrically pumped structure at room temperature, showing good agreement with the theoretical models. TPG is observed directly by measuring the nonlinear output-intensity growth with increasing input power, and by examining its dependence on the injected current for various-length waveguides. In supplementary experiments we monitored the effect of two-photon transitions on one-photon emission (OPE) [Fig. 1(d)] above the TPT point, which further validated the direct TPG measurements. The semiconductor  $p$ - $i$ - $n$  heterostructure based on AlGaAs layers was specially designed to optimize the tightly guided optical mode confinement to the active gain region, as well as the two-photon nonlinear interaction length. Since the two-photon transition probability is crystal momentum,  $k$ , dependent [18], the optimal active TPG layer of the semiconductor structure is designed to have a band gap slightly narrower than  $2\hbar\omega_p$ , where  $\omega_p$  is the photon angular frequency, enabling two-photon interaction with electrons at higher  $k$  values. The design results in larger TPG relative to the parasitic effects; the latter are primarily free-carrier absorption and second harmonic generation in AlGaAs [22]. This enables the observation of TPG, which could not have been achieved in the previous structure [21]. Moreover, the many-body effect of band gap renormalization [23] can be exploited to obtain larger two-photon coefficient values,  $\gamma_2$ , at TPG, compared to the absolute value at zero current (maximal TPA), due to the band gap dependence of  $\gamma_2$  [11].

In TPG medium, the spatial change in the light intensity  $I$  propagating in the  $z$  direction, neglecting higher order nonlinearities [14], is given by [17]

$$dI/dz = \Gamma\gamma_2' I^2 - \alpha I, \quad (1)$$

where  $\Gamma$  is the confinement factor of the waveguide,  $\alpha$  is the linear loss coefficient, and  $\gamma_2'$  is the semiconductor TPG coefficient given by [11,17]

$$\gamma_2' = \frac{8\pi\omega_p}{I^2} \sum_f \int \frac{d^2k}{(2\pi)^3} [F_c(k) - F_v(k)] \times \left| \sum_n \frac{\langle f|H|n\rangle\langle n|H|i\rangle}{E_n - E_i - \hbar\omega_p} \right|^2, \quad (2)$$

where  $F_c(k)$  and  $F_v(k)$  are the quasi-Fermi-Dirac distribution functions in the conduction and valence bands, re-

spectively, and indices  $f$ ,  $n$ , and  $i$  stand for the final, intermediate, and initial states accordingly.  $H = -\frac{e}{m}\hat{p} \cdot \hat{A}$  is the electron-radiation interaction Hamiltonian, where  $e$  is the electron charge,  $\hat{p}$  is the electron momentum operator,  $\hat{A}$  is the vector potential operator, and  $m$  is the electron mass, while energy conservation dictates  $E_f - E_i = 2\hbar\omega_p$ . Both  $\alpha$  and  $\gamma_2'$  depend on charge-carrier concentration  $n$ , where  $n$  dependence of  $\alpha$  stems mainly from free-carrier absorption and that of  $\gamma_2'$  from the separation of the quasi-Fermi levels  $E_{FC}$  and  $E_{FV}$  of the conduction and valence bands, respectively [Eq. (2)]. When the separation satisfies the two-photon population inversion condition  $E_{FC} - E_{FV} > 2\hbar\omega_p$ ,  $\gamma_2'$  becomes positive [Fig. 1(c)], resulting in TPG, while at lower carrier injection the gain is negative, corresponding to TPA. The solution of Eq. (1) for a device length  $L$  with an input intensity  $I_0$  is

$$I_{\text{out}} = I_0 e^{-\alpha L} / [1 - \gamma_2 I_0 (1 - e^{-\alpha L}) / \alpha], \quad (3)$$

where  $\gamma_2 \triangleq \Gamma\gamma_2'$ . Therefore, the output intensity exhibits concave dependence on input intensity for TPA ( $\gamma_2 < 0$ ), linear dependence on input intensity for TPT ( $\gamma_2 = 0$ ), and convex dependence on input intensity for TPG ( $\gamma_2 > 0$ ).

In our experiments, the structure was composed of a  $0.5 \mu\text{m}$  thick  $\text{Al}_{0.11}\text{Ga}_{0.89}\text{As}$  active layer having a band gap  $\sim 30$  meV smaller than  $2\hbar\omega_p$  for  $1.56 \mu\text{m}$  photons. The TPG structure was epitaxially grown on GaAs substrate [Fig. 1(e)], with cladding layers and a core layer comprising a highly confining single-mode slab waveguide in the growth direction. Lateral confinement was achieved by a ridge structure formed by wet etching to a depth of  $\sim 1.7 \mu\text{m}$ , yielding a confinement factor of  $\sim 0.6$ , which is more than an order of magnitude higher than the quantum well confinement factor in [21]. Facet reflectivity was reduced to increase the threshold current density of the undesired one-photon lasing to above  $8000 \text{ A/cm}^2 \mu\text{m}$  (corresponding to  $4000 \text{ A/cm}^2$  in our devices). The input laser was a mode-locked fiber laser source generating  $\sim 100$  fsec pulses at  $1560 \text{ nm}$  central wavelength,  $37 \text{ MHz}$  repetition rate, and up to  $40 \text{ mW}$  average power. The femtosecond laser pulse train was chopped at  $293 \text{ Hz}$  and coupled into the waveguide by a lensed fiber resulting in a  $2.5 \mu\text{m}$  spot size at a working distance of  $14 \mu\text{m}$ . The lensed fiber position was optimized using a piezoelectric nanopositioning system.

First, we observed TPA and TPG indirectly by monitoring the OPE for a  $800 \mu\text{m}$  long device using a lock-in detection scheme and a Si femtowatt receiver, in a setup similar to that described in [21]. Measurements of the reduction of OPE around a wavelength of  $800 \text{ nm}$  as a function of the input intensity and at various injected currents (Fig. 2) resulted in negative  $\gamma_2$  for low current injection, namely, TPA-induced enhancement in carrier density and in the OPE. With an increased current injection,  $\gamma_2$  becomes less negative reaching the TPT point at nearly  $1300 \text{ A/cm}^2 \mu\text{m}$ , above which  $\gamma_2$  becomes positive corresponding to TPG. The effect of TPA or TPG on OPE

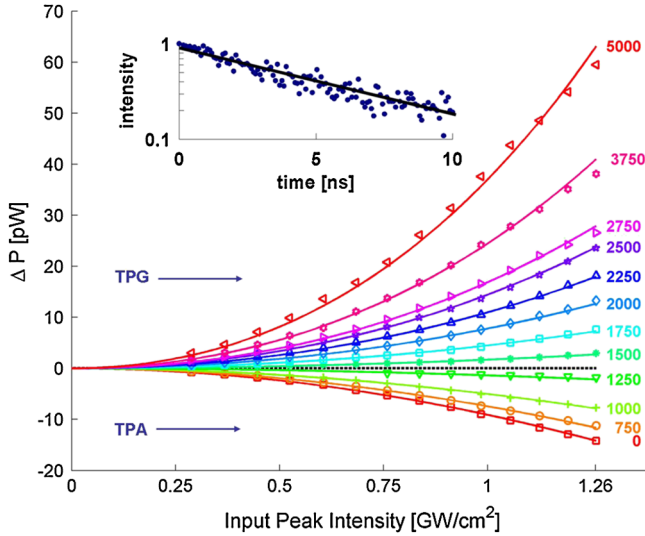


FIG. 2 (color online). Reduction in 800 nm OPE ( $\Delta P$ ) versus input light intensity at different current densities (in units of  $A/cm^2 \mu m$ ). Negative  $\Delta P$  values correspond to TPA-induced carrier density and OPE increase, while positive  $\Delta P$  values correspond to TPG-reduced carrier density and OPE decrease. Continuous lines represent theoretical fits according to  $\gamma_2 I^2$ . The inset is a time-resolved measurement of the TPA-induced OPE using a start-stop configuration of a Si single-photon detector with the pulsed laser. The semilogarithmic time histogram, presented in arbitrary units, shows an exponential decay with a  $\tau = 6.35$  nsec carrier lifetime.

behaves according to  $\gamma_2 I^2$ , in good agreement with our measurements (Fig. 2). At zero injection  $\gamma_2$  is  $-0.65$  cm/GW, similar to recently reported values [24], and it reaches  $\sim 2.7$  cm/GW for current density of  $5000 A/cm^2 \mu m$ , which is below the one-photon lasing threshold. To estimate reliably the charge-carrier concentration  $n = -\Gamma \gamma_2 I^2 \tau / \hbar \omega_p$  for a given structure and experimental conditions, the carrier lifetime  $\tau$  was measured by time-resolved TPA-induced OPE (Fig. 2 inset), employing a Si photon counter in a start-stop configuration with the input laser, yielding  $\tau = 6.35$  nsec—comparable to previously reported results [25]. The value of  $\gamma_2$  at maximal gain is about 4 times larger than its absolute value at zero current in agreement with the calculation considering band gap renormalization [11].

In order to observe TPG directly, we examined the highly nonlinear behavior of the amplification. Since the nonlinearity is more prominent for longer waveguides (Fig. 3 inset), we used 1.5 and 2.9 mm long waveguides. In this experiment the input 1560 nm laser was chopped and the output signal was detected using an InGaAs detector in a lock-in scheme through an iris positioned in the image plane to collect light mainly from the active region. TPA, TPT, and TPG measurements at various current densities were performed, yielding for the device length of 2.9 mm  $\gamma_2$  value of  $3.15$  cm/GW at charge-carrier concentration of  $\sim 3 \times 10^{18} cm^{-3}$  and linear loss of  $\alpha =$

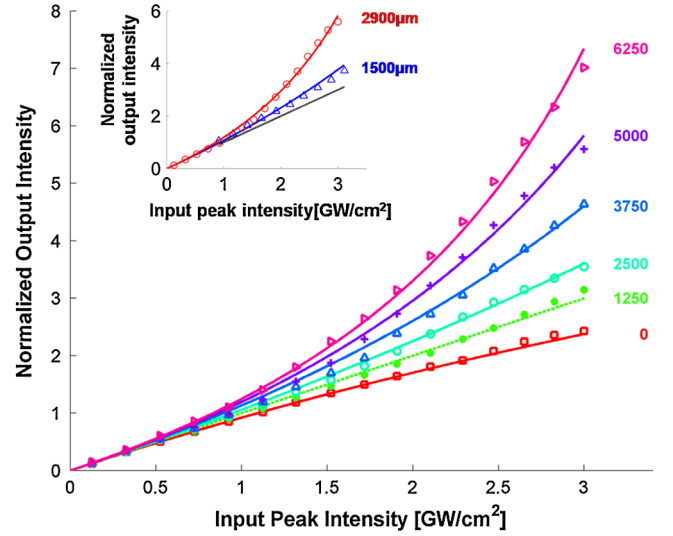


FIG. 3 (color online). Direct measurements of 1560 nm TPG for a 2.9 mm long waveguide at different current densities (in units of  $A/cm^2 \mu m$ ) normalized by the linear slope coefficient of each graph at low input powers. Continuous lines represent theoretical fits [by Eq. (3)] to the measured points. The inset compares the behavior of the TPG for two different waveguide lengths at  $\sim 5000 A/cm^2 \mu m$ .

$15.8 cm^{-1}$ . Since both the linear loss and the TPG increase with current, in order to demonstrate the nonlinear dependence on input intensity for different currents on the same footing, the output intensity is normalized by the linear slope coefficient at low input powers, such that the curve at transparency indicates  $I_{out} = I_{in}$  (Fig. 3). Therefore the effect of nonlinear two-photon gain on the  $I_{out}(I_{in})$  dependence is singled out. Transparency condition for all three different lengths was obtained at similar current densities.

In conclusion, we have observed and characterized in detail TPG in an electrically driven semiconductor structure for the first time, in good agreement with the theory. The nonlinear TPG is observed directly by examining the optical intensity of the amplified signal and indirectly by monitoring the reduction in OPE due to two-photon transitions above the TPT point. These results pave the way for the realization of miniature and efficient two-photon lasers, quantum-light sources, and integrable photonic devices for ultrashort pulse generation.

\*To whom correspondence should be addressed.

nevet@tx.technion.ac.il

- [1] P. P. Sorokin and N. Braslau, *IBM J. Res. Dev.* **8**, 177 (1964).
- [2] A. M. Prokhorov, *Science* **149**, 828 (1965).
- [3] M. O. Scully, K. Wodkiewicz, M. S. Zubairy, J. Bergou, N. Lu, and J. Meyer ter Vehn, *Phys. Rev. Lett.* **60**, 1832 (1988).
- [4] H. P. Yuen, *Phys. Rev. A* **13**, 2226 (1976).
- [5] F. Grosshans and P. Grangier, *Phys. Rev. Lett.* **88**, 057902 (2002).

- [6] J. Shapiro and G. Breit, *Phys. Rev.* **113**, 179 (1959).
- [7] S. Yatsiv, M. Rokni, and S. Barak, *Phys. Rev. Lett.* **20**, 1282 (1968).
- [8] M. M. T. Loy, *Phys. Rev. Lett.* **41**, 473 (1978).
- [9] D. J. Gauthier, Q. Wu, S. E. Morin, and T. W. Mossberg, *Phys. Rev. Lett.* **68**, 464 (1992).
- [10] O. Pfister, W. J. Brown, M. D. Stenner, and D. J. Gauthier, *Phys. Rev. Lett.* **86**, 4512 (2001).
- [11] C. N. Ironside, *IEEE J. Quantum Electron.* **28**, 842 (1992).
- [12] C. Z. Ning, *Phys. Rev. Lett.* **93**, 187403 (2004).
- [13] D. R. Heatley, W. J. Firth, and C. N. Ironside, *Opt. Lett.* **18**, 628 (1993).
- [14] N. Kaminski, A. Hayat, P. Ginzburg, and M. Orenstein, *IEEE Photonics Technol. Lett.* **21**, 173 (2009).
- [15] A. Hayat, P. Ginzburg, and M. Orenstein, *Nat. Photon.* **2**, 238 (2008); A. Nevet, N. Berkovitch, A. Hayat, P. Ginzburg, S. Ginzach, O. Sorias, and M. Orenstein, *Nano Lett.* **10**, 1848 (2010).
- [16] A. Hayat, P. Ginzburg, and M. Orenstein, *Phys. Rev. Lett.* **103**, 023601 (2009).
- [17] V. Nathan and A. H. Guenther, *J. Opt. Soc. Am. B* **2**, 294 (1985).
- [18] L. Costa, M. Betz, M. Spasenović, A. D. Bristow, and H. M. van Driel, *Nature Phys.* **3**, 632 (2007).
- [19] F. Boitier, A. Godard, E. Rosencher, and C. Fabre, *Nature Phys.* **5**, 267 (2009).
- [20] D. H. Marti, M.-A. Dupertuis, and B. Deveaud, *IEEE J. Quantum Electron.* **39**, 1066 (2003).
- [21] A. Hayat, A. Nevet, and M. Orenstein, *Phys. Rev. Lett.* **102**, 183002 (2009).
- [22] M. Ravaro, Y. Seurin, S. Ducci, G. Leo, V. Berger, A. De Rossi, and G. Assanto, *J. Appl. Phys.* **98**, 063103 (2005).
- [23] D. A. Kleinman and R. C. Miller, *Phys. Rev. B* **32**, 2266 (1985).
- [24] D. Duchesne, L. Razzari, L. Halloran, R. Morandotti, A. J. Spring Thorpe, D. N. Christodoulides, and D. J. Moss, *Opt. Express* **17**, 5298 (2009).
- [25] H. A. Zarem, J. A. Lebens, K. B. Nordstrom, P. C. Sercel, S. Sanders, L. E. Eng, A. Yariv, and K. J. Vahala, *Appl. Phys. Lett.* **55**, 2622 (1989).